Princeton Plasma Physics Laboratory

Alignment of the Thomson Scattering Diagnostic on NSTX

B.P. LeBlanc and A. Diallo

October 2013

PRINCETON
PLASMA PHYSICS
LABORATORY

Princeton Plasma Physics Laboratory
Report Disclaimers

PPPL Report Availability

Princeton Plasma Physics Laboratory:

http://www.pppl.gov/techreports.cfm

Office of Scientific and Technical Information (OSTI):

http://www.osti.gov/bridge

Related Links:

U.S. Department of Energy

Office of Scientific and Technical Information

Fusion Links

Alignment of the Thomson scattering diagnostic on NSTX

B. P. LeBlanc[a][*] and A. Diallo[a]

[a]*Princeton Plasma Physics Laboratory*,
POB 451, Princeton, NJ, 08543, USA
E-mail: leblanc@pppl.gov

ABSTRACT: The Thomson scattering diagnostic can provide profile measurement of the electron temperature, T_e, and density, ne, in plasmas. Proper laser beam path and optics arrangement permits profiles $T_e(R)$ and $n_e(R)$ measurement along the major radius R. Keeping proper alignment between the laser beam path and the collection optics is necessary for an accurate determination of the electron density. As time progresses the relative position of the collection optics field of view with respect to the laser beam path will invariably shift. This can be kept to a minimum by proper attention to the physical arrangement of the collection and laser-beam delivery optics. A system has been in place to monitor the relative position between laser beam and collection optics. Variation of the alignment can be detected before it begins to affect the quality of the profile data. This paper discusses details of the instrumentation and techniques used to maintain alignment during NSTX multi-month experimental.

KEYWORDS: Thomson scattering; Alignment; Density.

---

[*] Corresponding author.

Contents

1. Introduction

Incoherent Thomson scattering (TS) is a standard diagnostic often required for the study of plasma physics: it is a must-have for magnetic fusion research, where it provides profile measurement of the electron temperature, T_e, and density, n_e. Proper laser beam path and optics arrangement enables profile $T_e(R)$ and $n_e(R)$ measurement along the major radius R. Since the temperature information resides in the spectral spread, the T_e measurement simply requires an acceptable S/N ratio of the scattered signal distributed in an adequate number of relatively calibrated spectral channels,. But the determination of the $n_e(R)$ is more demanding. Besides the requirement for $T_e(R)$, the diagnostic must also be absolutely calibrated, well aligned and remain so for a period commensurate with the duration of the experimental research program, which for NSTX[1] is typically six months. Fine alignment and absolute calibration are usually done using Rayleigh and/or Raman scattering[2]. We will refer to this alignment as the "calibration alignment". Maintaining the calibration alignment is a demanding task that needs to be met daily in order for the $n_e(R)$ profile information – shape and gradient – to be meaningful. While precautions in the design of the laser delivery and collection optics can enhance pointing and viewing stability, alignment drift from the calibration alignment will invariably occur over long time. This paper discusses details of the instrumentation and technique used to quantify the calibration alignment and small drift around it. It also discusses how we maintain the day-to-day operational alignment sufficiently close to the calibration alignment as to preserve the quality of the $n_e(R)$ data.

2. Alignment channels

2.1 Hardware

The MPTS collections optics comprises thirty-six fiber bundles, each composed of 21 fibers of nominal 500-μm diameter. Each bundle input end is arranged in three closely packed lines of respectively 8, 7 and 6 fibers, resulting in a dove-tail cross-section. The two fibers located at the extreme vertices are reserved for alignment measurement and monitoring. The bundle tails are arranged in an alternating up-and-down fashion, as illustrated in Fig. 1. It shows images of the fiber bundle array along the laser beam path, although for simplicity, only six bundles are visible and optics magnification effects have been neglected. A vectorized line represents the

laser-beam center; the misalignment of the beam with respect to the bundle array axis has been exaggerated for this discussion. Half of the alignment fibers view above the laser line and the other half views below it. The alignment fibers viewing the top are assembled in three groups corresponding to segments along the laser beam path: inner edge, middle and outer edges. The alignment fibers viewing the bottom are arranged similarly. The output ends of the top and bottom alignment fibers of each segment are assembled in separate bundles. Four of the resulting six alignment fiber bundles are instrumented, corresponding to the inner and outer laser path segments. This optical arrangement provides a means of determining the relative position of the laser beam(s) with respect to the field of view of the collecting optics.
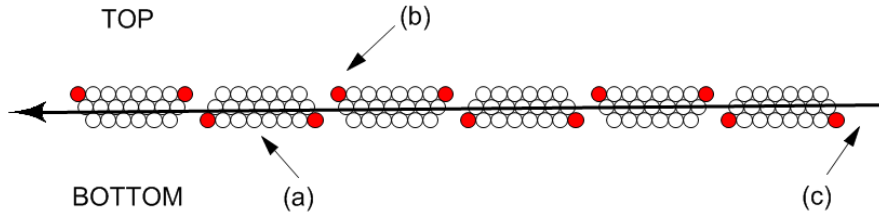

Fig.1: Alignment measurement: Each bundle (a) is made of 21 fibers, of which 2 are reserved for alignment measurement (b). The long arrow represents a laser beam (c).
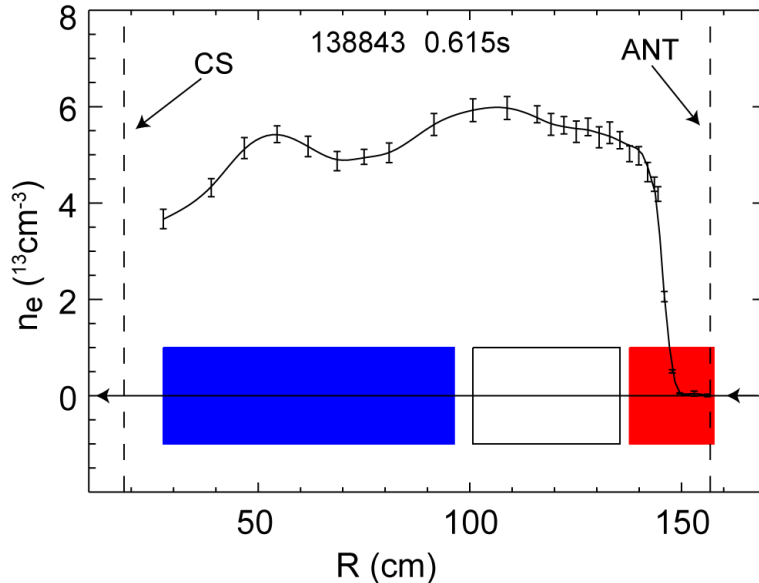

Fig.2: Typical H-mode $n_e(R)$ profile and location of alignment segments: inner, middle and outer segments. Also shown are the wall of the center stack (CS) and the location of the HHFW antenna limiter (ANT).

One can see in Fig.2 a $n_e(R)$ profile for a typical NSTX H-mode plasma. The three alignment sampling segments are indicated with rectangles. While the horizontal span of the rectangles represents the major radius coverage, their vertical height is non-physical and has been drawn to help visibility. The center stack wall and HHFW-antenna limiter are also shown. The NSTX TS system covers over 90% of the machine aperture on the horizontal midplane, which has a geometric center $R_{GM} \approx 85$ cm. The light emanating from each alignment bundle is

collimated and sent through a bandpass filter before being focused on an APD detector. The central wavelength of bandpass filter of the top-and-bottom pairs has been selected such that it will collect TS light even at low T_e and also collect light during Raman scattering calibration done with nitrogen gas. Bearing in mind that the laser wavelength is 1064 nm, the central filter wavelength for the inner segment has been set to 1048 nm, since this segment views inside the inner edge pedestal where T_e should be between 0.2 and 1.0 keV. The filter of the outer segment has been set to 1058 nm in view of the lower T_e expected in the plasma edge and boundary regions. We will refer to this arrangement as the four "alignment channels". The configuration is schematized in Fig. 3. A figure of merit for quantifying the alignment can be defined as "A" the top-the-bottom ratio of the alignment signals, respectively in the inner and outer alignment segments. Hence we will have A[in]=AligSign[in,top]/AligSig[in,bot], where AligSign[in,top] is the signal from the alignment channel at the inner top and AligSig[in,bot] is the signal from the alignment channel signal at the inner bottom. A similar parameter for the outer edge, A[out], can be defined.

```
        TOP                    TOP
        1048 nm                1058 nm
CENTER                                        OUTER
STACK   ◄───────────────────────────────      EDGE
        1048 nm                1058 nm
        BOTTOM                 BOTTOM
```

Fig.3: The four alignment channels

Through the course of time, the MPTS diagnostic has undergone many upgrades, and the configuration discussed here includes twenty six-filter polychromators and ten four-filter polychromators and two 30-Hz Nd:YAG lasers. The two lasers pulse at different times in order to increase the time resolution. Each laser's alignment can change independently from the other, hence in the following, separate alignment data will be shown for each.

2.2 Alignment scan

One way to document the system behavior in the vicinity of the calibration alignment is to proceed to controlled scans of the optical components around the calibration alignment with Raman scattering. In the present case, this would involve scans of the collection optics, or of the last two mirrors of the laser-beam delivery optics. This work is usually done just prior to Raman calibration. We can see in Fig4 the results of such a scan, where the elevation of the collection optics field of view is scanned relative to the laser path, with 50 Torr of nitrogen in the vacuum vessel. The figure shows the scattered light signal though the 1058-nm spectral channel for a subset of twenty radial channels and two laser beams. The nine first channels labeled PH1 are shown in the top line. The left and right columns correspond to laser 1 and 2 respectively. Channels corresponding $R < R_{GM}$, are shown with dashed lines and channels with $R > R_{GM}$ are shown with solid lines. The horizontal axis is the vertical adjustment V of one of the legs of the kinematic mount that supports the collection optics; V=0.0 corresponds to the calibration alignment. This vertical adjustment has been designed to keep the field of view horizontal. One can see that for large values of R (solid lines), the height of the field of view of the collection optics is well matched to the size of the laser beams: it takes about $\Delta V= 0.6$ cm for the optics to scan through the laser beam diameter. One can also see that the calibration set point, V=0.0, has been chosen as a compromise in view of the small tilt of the collection optics field of view and the laser beam path. The match between the laser beam size and the field of height is not as

good for lower R channels, in part because the collection optics is slightly out of focus at the inner edge and also because of details of the collection optics mirror configuration.
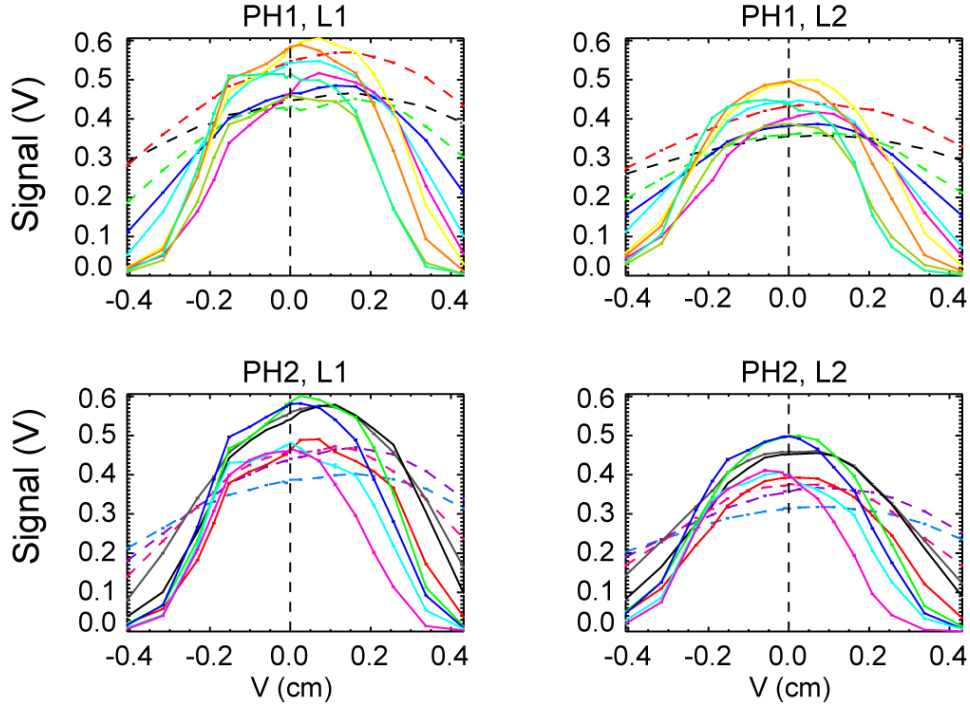

Fig.4: Variation of Raman signal during collection optics vertical scan. The wavelength bandwidth center is at 1058 nm. The calibration alignment is indicated by the vertical dashed line.

We can see in Fig.5 a plot of the alignment channel signals for the same Raman scattering data shown in Fig. 4. The left column corresponds to the inner alignment segment – blue bloc – and the right column corresponds to the outer segment – red bloc – shown in Fig. 2. Looking at the upper right panel, one sees that the calibration alignment is fairly well centered for the outside alignment segment. The bottom and top alignment signals are nearly mirror images of each other around the calibration set point, V=0.0, although laser 1 is better aligned than laser 2. One can also see that the alignment is not as perfectly "balanced" on the inside. The choice of the calibration alignment is actually a compromise that stems from hardware limitations, which preclude having a perfect alignment throughout. Better centering has been given to the outer edge because of the tighter match between the laser and collection optics mentioned in Fig. 4, and also because of the importance of the outer edge in the NSTX research program. The fact that the inner edge is not as well centered as the outer edge for the calibration alignment does not really matter as long as we are able to keep the day-to-day alignment the same as the calibration alignment. This a task that can be accomplished by making use the alignment quantifier parameter A mentioned above. Since A varies rapidly, over a few orders of magnitude for the vertical scan, it is preferable to display its logarithm as it is done in the two bottom panels of Fig. 5. The bottom left panel shows the A[in] against vertical setting V of the scan. Consistent with comments made just above, laser 1 appears to have a sharper alignment than laser 2: the A[in] for laser 1 has a greater gradient against V.
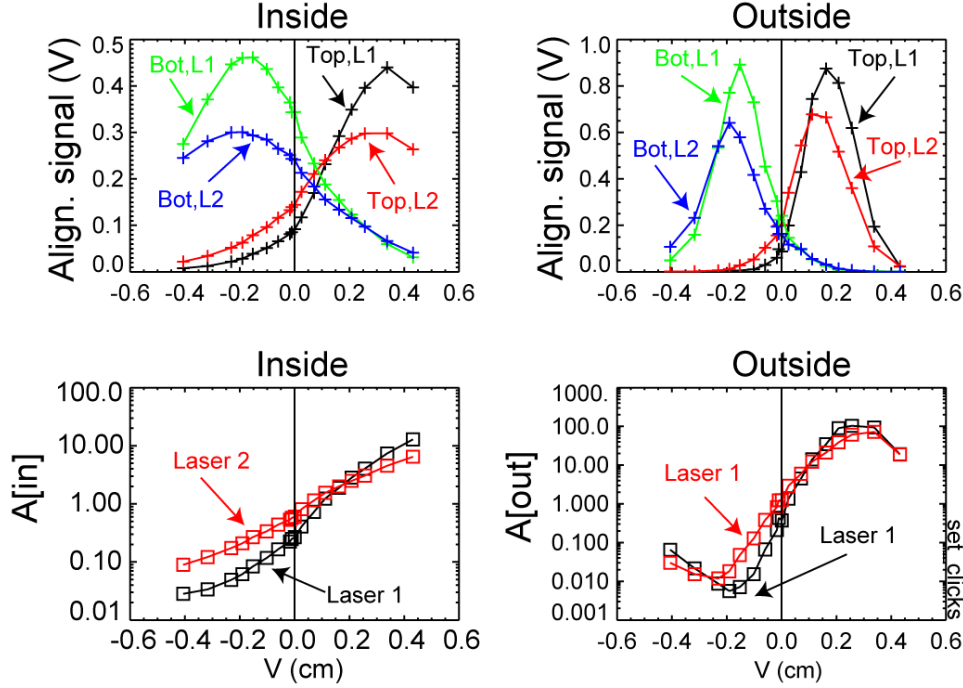
Fig. 5: Collection optics vertical scan around calibration alignment at V=0.0. Top panels: alignment channel signals for inner and outer segments. Bottom panels: alignment parameter A. Data shown for laser 1 and 2.

2.3 Experimental example

One can see in Fig. 6 a time evolution of the four alignment channel signals for the same high power NSTX discharge shown in Fig. 2.The figure-6 panel arrangement corresponds to what is shown in Fig. 3. The plasma lasted until 1.05 sec, but times prior to 0.1 s are ignored in the alignment analysis. The time varying alignment channel data is concatenated into single time alignment signal values, in order to assess the average alignment during the discharge. One can then compute the alignment ratio parameters A[in] and A[out] and compare them with the collection-optics vertical scan data set in order to determine the offset of the experimental alignment relative to the calibration alignment. This is done by interpolating the experimental A values onto the vertical scan results to extract the experimental V values for the inner and outer segments. This calculation is presented in Fig. 7. The inner edge and outer alignment data is shown respectively in the top and bottom panels. The solid lines with "x" symbols correspond to the vertical scan data for laser 1 and laser 2 discussion previously. The squares correspond to the experimental points. The A parameter interpolation over the vertical scan data reveals this experimental alignment to be good, with $-0.007 < \Delta V < 0.08$ cm over all. Please note the six-fold reduction in V span on the horizontal axis in Fig. 7 compared to Fi. 5.
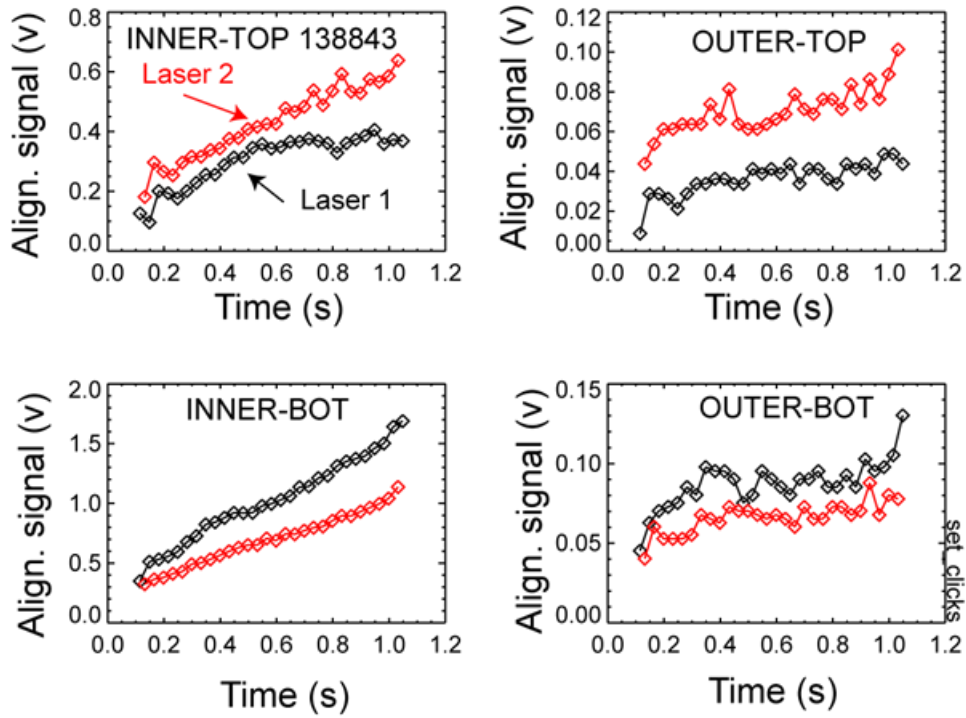
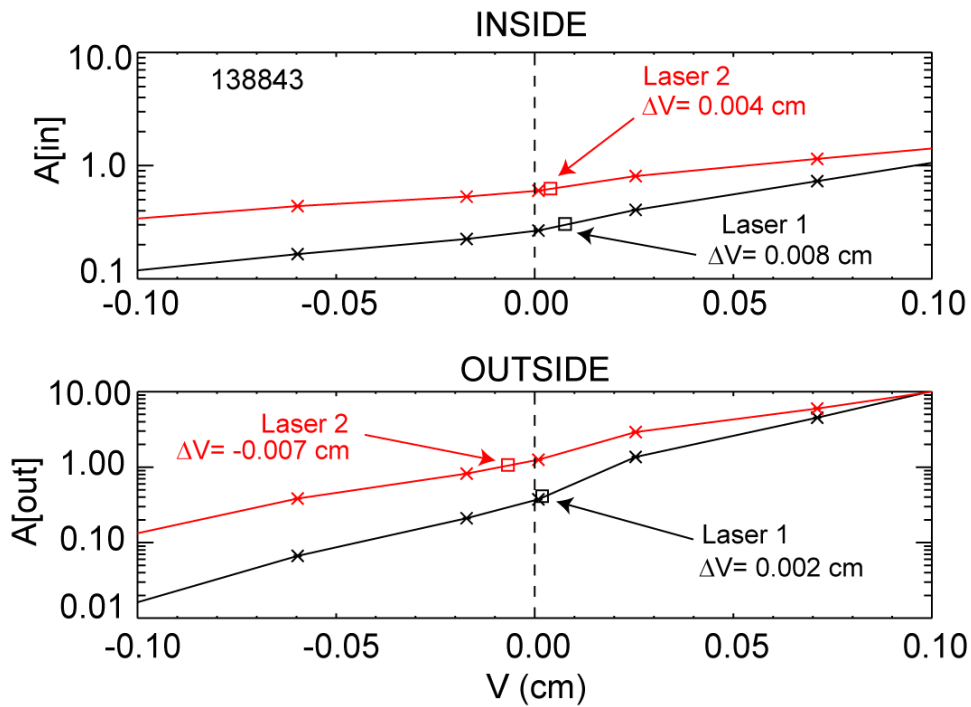Fig. 6: Alignment channel signals for a NSTX high performance discharge.

Fig. 7: Squares indicate inner and outer alignment parameter A for discharge 138843.

3. Discussion

The alignment channels constitute a powerful tool permitting us to evaluate quantitatively the alignment of the two individual laser beams and the collection optics. It is observed experimentally that alignment drift almost always involves both lasers moving together in the same direction. There are only three optical elements that could be responsible for this effect, namely: the collection optics itself and the last two mirrors of the laser delivery optics, which reflect both beams. These two mirrors are many meters away from NSTX and usually a correction is applied to the farthest mirror. While an additional goal could have been to recover a measurement made when the system was significantly far from the calibration alignment, it has proven impractical without the data from the middle alignment segment. The difficulty comes from the details of the laser beam profiles convoluted with the profile of the viewing optics vertical extent. As a result, our approach has been to keep the alignment always close to the calibration alignment, in which case there is no need to correct the $n_e(R)$ profile for alignment effects. Practically, we keep ΔV below ± 0.05cm.

Acknowledgments

References

[1] M. Ono, S.M. Kaye, Y.-K.M. Peng, et al., Nuclear Fusion 40, 557 (2000).
[2] B.P. LeBlanc, *et. al.* Rev. Sci. Instrum., **79**, 10E737 (2008)